



Corrugated Winglets Efficiency: A Numerical Study

Mohamed Hussain Farook^{1,*}, Vishnu Kumar Gettin Chitharanjan¹

¹ Department of Aeronautical Engineering Hindustan Institute of Technology and Science, Padur, Chennai, Tamil Nadu 603103, India

ARTICLE INFO

Article history:

Received 20 September 2024

Received in revised form 21 November 2024

Accepted 19 December 2024

Available online 28 February 2025

Keywords:

Lift; drag; SolidWorks; Ansys fluent; CFD

ABSTRACT

This research compares the efficiency of raked and blended wingtip devices performance by modifying the winglet tip. The study validates these modifications against the baseline wing's aerodynamic properties. The simulations reveal a strong correlation between the size of the tip vortex and the wing's lift, drag and pitching moment. According to the study, winglet tip optimisation is crucial for maximising lift and reducing drag. Corrugated tips demonstrated the best aerodynamic performance, enhancing both flight range and endurance. The number of winglet research papers has shown the best of raked and blended winglet gives 5% more lift coefficient than the conventional wing. According to the present research, it is noted that the winglet with corrugation gives 2% more than the exiting raked and blended. Comparatively the corrugation winglets give totally 7% than the conventional wing. By using corrugated winglets will reduce the drag in the flight range without affecting the lift.

1. Introduction

According to Anderson [1], the lift generated by a wing can be understood by analysing the flow over its entire span to achieve a three-dimensional lift distribution. This theory models the wing as a series of infinitely small sections, each producing lift and contributing to the overall aerodynamic behaviour of the wing. The lift distribution along the span of the wing is not uniform; it varies from root to tip, typically peaking near the root and tapering off towards the tips. Furthermore, the tip vortices, observed near the wingtips, as illustrated in Figure 1. Whitcomb [2], who conducted an experimental study on the efficiency of a wing tip sail, contain the oldest study on the usefulness of tip devices in lowering the drag brought on by lift. Various wingtip device configurations have demonstrated potential aerodynamic benefits, each offering improvements in areas such as lift, drag and fuel efficiency. However, McLean [3] comprehensive studies that account for all relevant variables such as flight conditions, aircraft design and operational efficiency have yet to identify any single configuration as having a definitive overall advantage. Consequently, the optimal choice of wingtip device may depend on specific use cases and operational priorities. Unless it exceeds a gate-clearance restriction or necessitates costly strengthening of the shear webs of an existing wing, the least expensive option is frequently a raked tip extension. With appropriate design, the effect of

* Corresponding author.

E-mail address: hussainiman07@gmail.com (Mohamed Hussain Farook)

wingtip vortices can be significantly decreased. Simulations using the Reynolds-Averaged Navier-Stokes equations with the $k-\omega$ SST turbulence model were conducted to analyse vortex structures and aerodynamic characteristics of the wings. Results indicate that multi-tipped winglets are most effective in dispersing vortex energy and reducing drag, with the multi-tip-3 winglet providing the best lift-to-drag ratio, optimizing flight range and efficiency. While more tips increased lift, the rise in frictional drag due to greater surface area was a limiting factor. Winglets were most beneficial on wings with moderate aspect ratios, particularly around 10 [4]. It discusses the strengths and limitations of models like the Reynolds-Averaged Navier-Stokes (RANS), Large Eddy Simulation (LES) and Direct Numerical Simulation (DNS) [5-7]. Because it can more readily maximise the vertical extent at the tip, a nonplanar split-tip geometry outperforms both the winglet and box-wing geometries for the same span wise and vertical bound constraints. All of the optimised geometries' performance is confirmed on refined grids with 88–152 million nodes. The following is a list of some intriguing findings from the optimization studies about induced drag. We point out that these findings might only hold true for inviscid flows. Furthermore, in certain situations, the designs might have been constrained by the parameterizations that were selected [9]. The book emphasizes the importance of choosing the appropriate model based on the specific flow characteristics, computational resources and accuracy requirements. RANS models, particularly $k-\epsilon$ and $k-\omega$, are highlighted for their efficiency in engineering applications, while LES and DNS offer higher accuracy but at a greater computational cost. The text serves as a critical reference for selecting and implementing turbulence models in CFD simulations. Tests were conducted in a wind tunnel at Brunel University [13], examining 25 serrated leading edges with varying wavelengths (λ) and amplitudes (h) at Reynolds numbers from 0.2 to 0.6 million. Results indicate that serrations with larger amplitudes (h) significantly reduce noise by up to 9 dB, while smaller amplitudes can increase noise at high frequencies. The noise reduction effectiveness depends on both λ and h , with designs featuring large values of both performing best. Curved serrations demonstrated superior performance, reducing noise by an additional 5 dB compared to straight serrations, due to an increased "effective" amplitude.

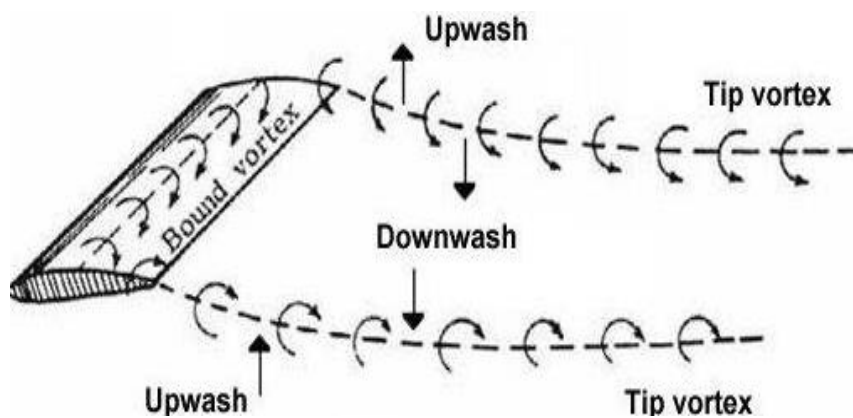


Fig. 1. Secondary flows cause tip vortices

Truncated trailing edges generate significant vortex shedding [14], increasing both lift and drag, but reducing the overall lift-to-drag ratio. Sharper serrations (with a smaller chevron angle, ϕ) reduce vortex shedding energy and improve lift-to-drag ratios. Fractal or multiscale serrations, which replicate these patterns at smaller scales, were also explored. Results show that broad chevrons ($\phi \approx 65^\circ$) increase vortex shedding, while sharper chevrons ($\phi \approx 45^\circ$) decrease it, leading to improved aerodynamic performance. For the standard transport aircraft wing-body of the DLR-F4 [15], the wing structural stress is examined. An alternative approach to a morphing winglet is presented based on

the analysis of the impact of can't angle. This approach mathematically parameterizes the concept of a curved winglet. We propose the use of variable cant angle winglets on the Onera M6 wing [16], which could potentially improve aircraft performance by reducing lift-induced drag across various angles of attack. Using computational fluid dynamics analysis, we examine how varying the cant and sweep angles of winglets affects the performance of a benchmark wing at Mach 0.8395. Our findings indicate that adjusting the cant angle may boost aerodynamic performance across different angles of attack. In comparison to other arrangements [17], the region around the wingtip area is smaller when secondary flow is generated utilizing the front wingtip barrier. Additionally, the measurement of pressure on the top surface that has a forward wingtip fence demonstrates that pressure is still rather high compared to the others.

The wing continues to travel with a constant linear velocity while the leading-edge vortex forms and sheds into the wake [18]. Similar results are obtained for the sweeping motion at the $Re=34000$ and at high angles of attack using flat plate and corrugated wings, which is in line with earlier study on flapping insects at the $Re=3500$. The force coefficients differ very little when the flat plate, profiled and corrugated wings are compared in sweeping action. The impact of Wavy Leading Edge (WLE) by Rohmawati *et al.*, [19] on experimental and numerical NACA 0018 profile. The results demonstrate that in a stable condition, the WLE on the taper wing has a higher advantage to control the stall. The WLE wing with $AR=7.9$ and $TR=0.3$ has the best lift coefficient and pressure distribution, which is another amazing finding. The numerical calculations are performed using the large eddy simulation (LES) method by Ilie *et al.*, [20]. To fabricate a NACA 2412 air foil section for experimental testing [21], the wing, with a 230 mm chord length and 305 mm width, was printed in three hollow sections and equipped with surface holes for pressure measurement using a multi-manometer. The experimental results were compared with CFD simulations conducted using ANSYS Fluent. The paper provides detailed insights into the design, fabrication, setup, costs and student learning experiences, along with tutorials for replicating the experiment and CFD simulations. It also assesses student engagement and the learning process.

The simulation results also show that the best way to improve the NACA inlet performance is to line up the height of the vortex generator with the thickness of the local boundary layer. The impact of the winglet is shown to depend on the wing's aspect ratio ($AR = 10, 15, 19.6$) by Zhang *et al.*, [24]. The shear layer [25] that passes through the serration array alters the surface pressure distribution over the upper surface, which has a negative effect on aerodynamic performance. Furthermore, it is discovered that serrations raise the degree of turbulence in the downstream flow. The presence of serrations upstream in the flow increased the turbulent momentum transfer near the trailing edge and affected the mechanisms involved in the formation of the separation vortex and its subsequent development over the upper surface of the wing. We compare the aerodynamic efficiency of single- and double-winglet designs. According to the early findings, the double-winglet increases the lift coefficient and decreases tip vortex production [26], which enhances the wing's aerodynamic performance. The configuration with $h=64$ mm, $\beta = 20$ degrees and $d=20$ mm yields the most notable improvement in the NACA inlet's performance, according to the CFD simulations. The achieved mass flow ratio is 0.7196 and the Ram recovery ratio is 0.7812. In comparison to the typical NACA inlet, both values show increases of 31.23% for the Ram recovery ratio and 14.72% for the Mass flow ratio. An analysis was conducted to assess the sensibility between the goal function and the design variables. While this study highlights the aerodynamic advantages of corrugated winglets, referencing additional research on similar and novel winglet designs can further validate the findings. In order to ascertain the lift distribution along the NACA 4415 wing span and to obtain the percentage errors between the CFD method and the Schrenk Approximation method. These procedures and actions could lead to mistakes in the outcome because of unintended consequences. However, this

study is fully completed and the indicated error between the two methods is roughly 13% for the lift coefficient and 3% for the lift force [27]. The study emphasizes by Arafat *et al.*, [28] how crucial it is to use sophisticated hybrid models, such as DDES, for precise aerodynamic predictions, especially in situations with high Reynolds numbers and notable flow separations. Although RANS works well for forecasting general aerodynamic performance, it is not very good at identifying intricate unsteady flow patterns, which are essential for accurate lift and drag calculations. The accuracy of aerodynamic simulations can thus be greatly increased by incorporating DDES into the design and analysis of small city vehicles, which will aid in the creation of more effective and ecologically friendly urban transportation options. The literature already discusses the development and performance of various wingtip devices, such as those by Whitcomb [2], who first examined wingtip devices to reduce drag. His work serves as a foundational point for much of the current research in winglet design. Additionally, studies like those by McLean [3] and Narayan *et al.*, [4] emphasize the importance of optimizing winglet geometry for improved aerodynamic performance strengthens the findings, the study could draw further comparisons between the current results and existing winglet performance data, particularly in terms of drag reduction and lift enhancement. For instance, earlier works are taken from [15,18,24] investigated different winglet designs such as the Wavy Leading Edge (WLE) and other morphing or variable cant angle winglets, which show similar trends in improving aerodynamic efficiency. These studies provide context for how various design alterations, including corrugation, influence key performance factors like lift, drag and tip vortices. Further analysis of how the corrugated winglets compared to more traditional or blended winglet designs can be better situated within these frameworks.

Types of wings with and without winglets characteristics is discussed in the literature review. The literature survey does not discuss winglet modification of Blended, raked type which is presently used in most of the commercial aircrafts. The aerodynamic effect and turbulence interaction of combining multi winglets is yet to be analysed. There is a scope of improving the winglets by modifying its shapes which is taken in the present study by comparing with previous literatures.

2. Methodology

2.1 Geometry Modelling

To achieve a high aspect ratio, wing was designed with a span of 3 meters, a chord length of 0.25 meters at the root and a chord length of 0.2 meters at the wingtip. The wing also features a blended winglet with a height of 0.15 meters. This geometry was modelled using SolidWorks software are taken from the previous study by Narayan *et al.*, [4] and Abbott *et al.*, [8]. The resulting wing area is calculated to be 0.6 square meters. It is worth noting that most studies in this field utilize a similar approach to design geometry. The NACA 2412 air foil was selected for this model, with a flow velocity of 40 m/s. Corrugation was introduced at the tips of the raked and blended winglets, referred to as CRW (Corrugated Raked Winglet) and CBW (Corrugated Blended Winglet), respectively.

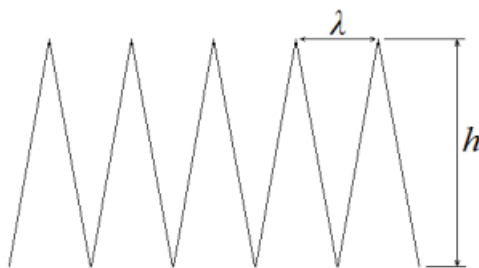


Fig. 2. Wavelength λ and amplitude height $2h$ of corrugation

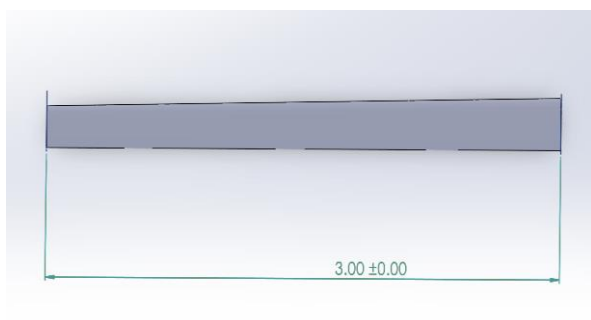
The winglets with wavelength and amplitude, as shown in Figure 2, are subsequently affixed to the baseline wing. Fuel savings are significant enough to maintain interest in developing a winglet-equipped aircraft from the start. The span of the winglets in this study is set to 10% of the baseline wingspan, a value supported by previous research from various authors [2,10,11], which suggests using a span between 10% and 20% of the wingspan for optimal winglet design.

In the final stages of the investigation, the raked winglets with sweep angle 26° from the previous study Halpert *et al.*, [12] and blended cant angle 30° have comparable geometric characteristics as shown in Table 1, which helps to measure the performances.

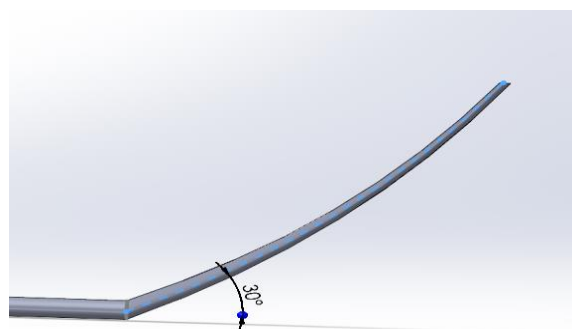
Table 1
 Wing and winglet design geometry

S. No:	Wing	Cant Angle (θ)	Sweep Angle (ϕ)	Wavelength (λ)	Amplitude height ($2h$)
1.	Baseline	-	-	-	-
2.	Raked	-	26.25°	-	-
3.	Blended	30°	-	-	-
4.	CRW	-	26.25°	15mm	50mm
5.	CBW	30°	-	15mm	50mm

The modified raked and blended winglets with dimensions as shown in Figure 3 are implemented using rectangular domain for the simulation.



(a)



(b)

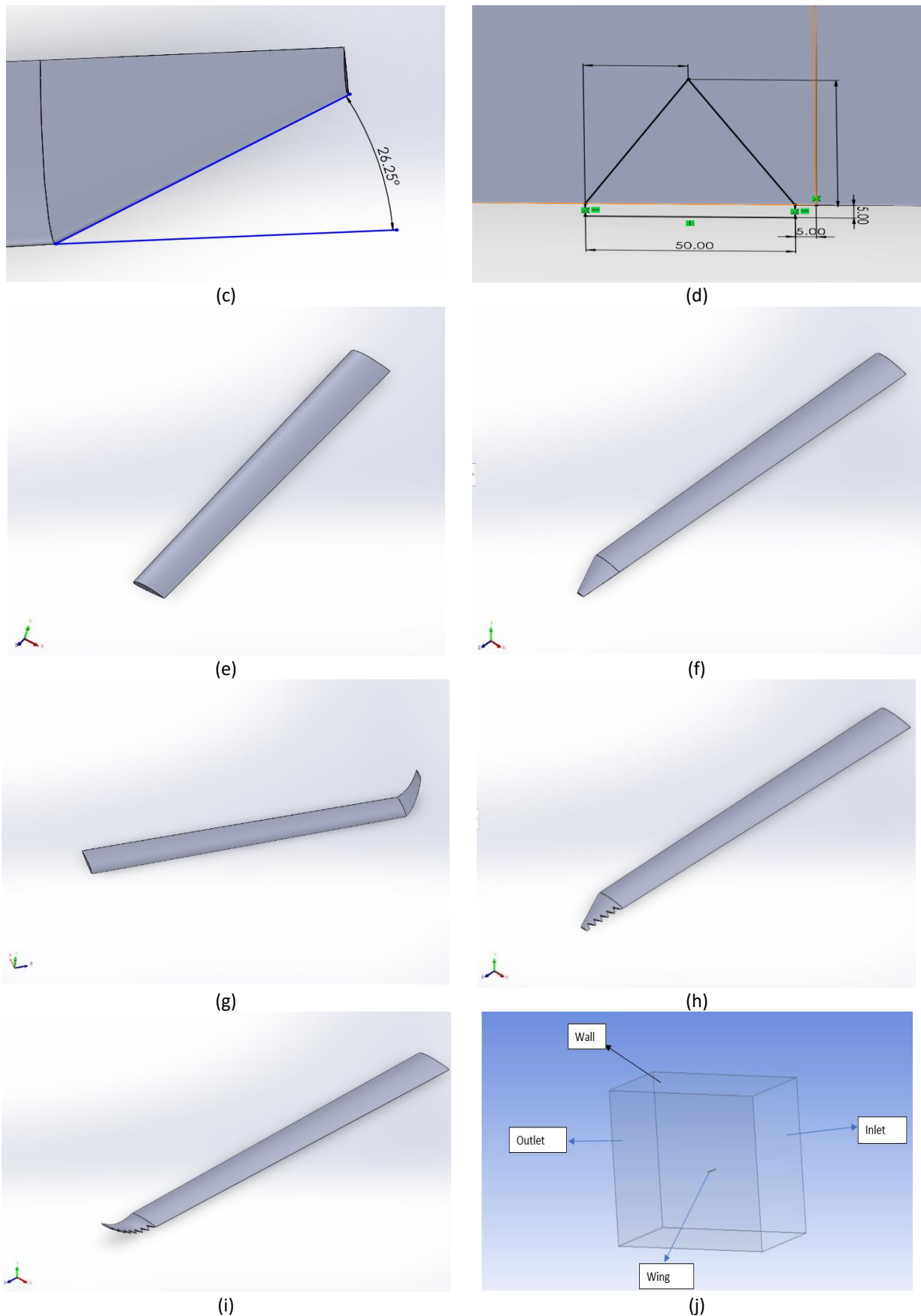


Fig. 3. The geometry model of wing and domain (a) wingspan (b) cant angle (c) sweep angle (d) corrugation dimension (e) conventional (f) Raked winglet sweep angle (g) Blended winglet (h) CRW (i) CBW (j) Rectangular domain

2.2 Meshing Generation

Tetrahedral elements are utilized to create the mesh. The mesh evolves from an initial 0.8 million elements to a final 1.6 million elements, covering coarse, medium and fine mesh configurations. It is observed that 1.5 million elements or more only gives impact in the lift and drag coefficient performance. This refinement process continued until all forces were accurately captured, with further mesh refinement depicted in Figure 4.

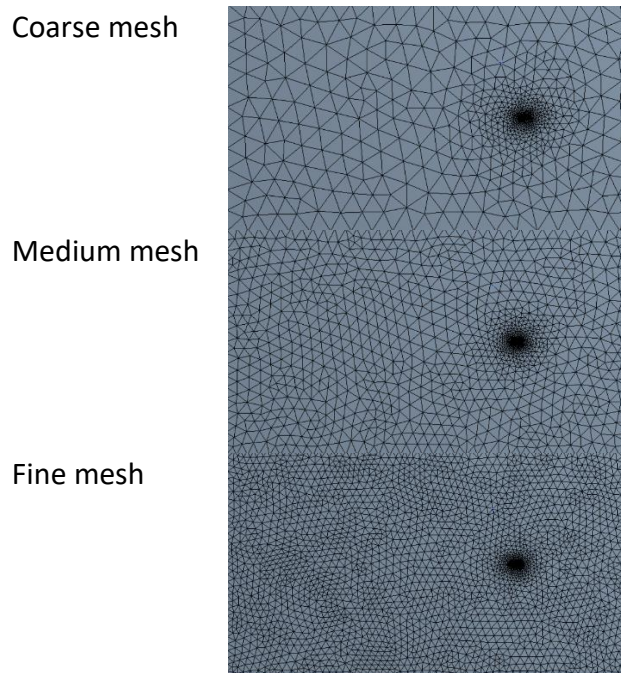


Fig. 4. coarse, medium and fine mesh of the domain

Consequently, for the present study, the converged grid was selected from a domain comprising 1.6 million components, as detailed in Table 2. Various wing geometries also underwent similar mesh-independent testing.

Table 2

Mesh convergence study

Velocity	Meshing	C_L at AOA 8	C_D at AOA 8
40 m/s	Mesh A (0.8 million elements)	1.0126	0.0168
	Mesh B (0.9 million elements)	1.0184	0.0159
	Mesh C (1.0 million elements)	1.0296	0.0597
	Mesh D (1.5 million elements)	1.0468	0.0649
	Mesh E (1.6 million elements)	1.0462	0.0647

The grid independent study was carried out at angle of attack 8° with velocity 40 m/s and the 1.6 million elements were commonly chosen after the coefficient of lift and drag was similar in that elements as shown in Figure 5. The lift and drag variation for the other mesh size has huge variation. The mesh convergence study as shown in Table 2 shows incremental improvements in the lift coefficient as the mesh is refined. Providing statistical metrics, such as the standard deviation or error bars, would clarify how much of this variation is due to computational approximation and help validate the grid independence of the results.

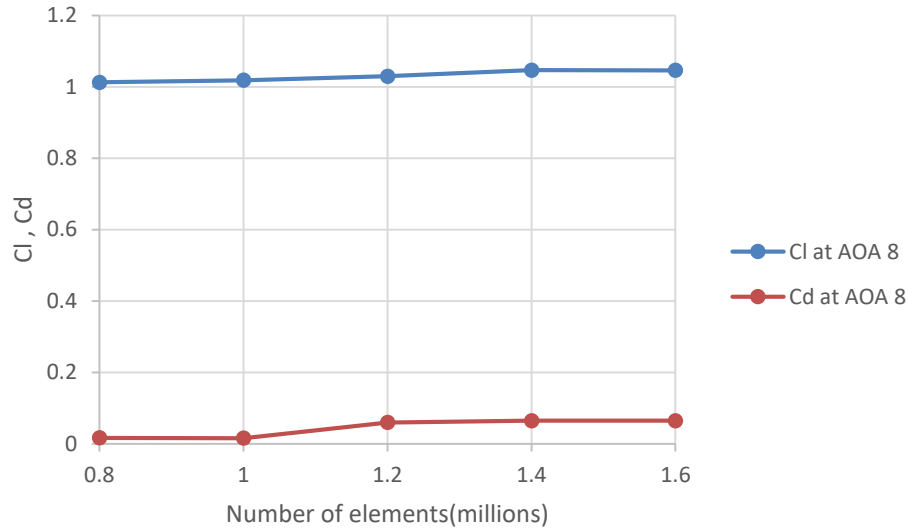


Fig. 5. Variation coefficient of lift and drag at AOA 8° vs grid refinement

An inflated structured sub-mesh was then placed around the grid to enable an appropriate boundary layer resolution. Figure 6 shows an illustration of the wall Y-plus distribution for the baseline model without winglets.

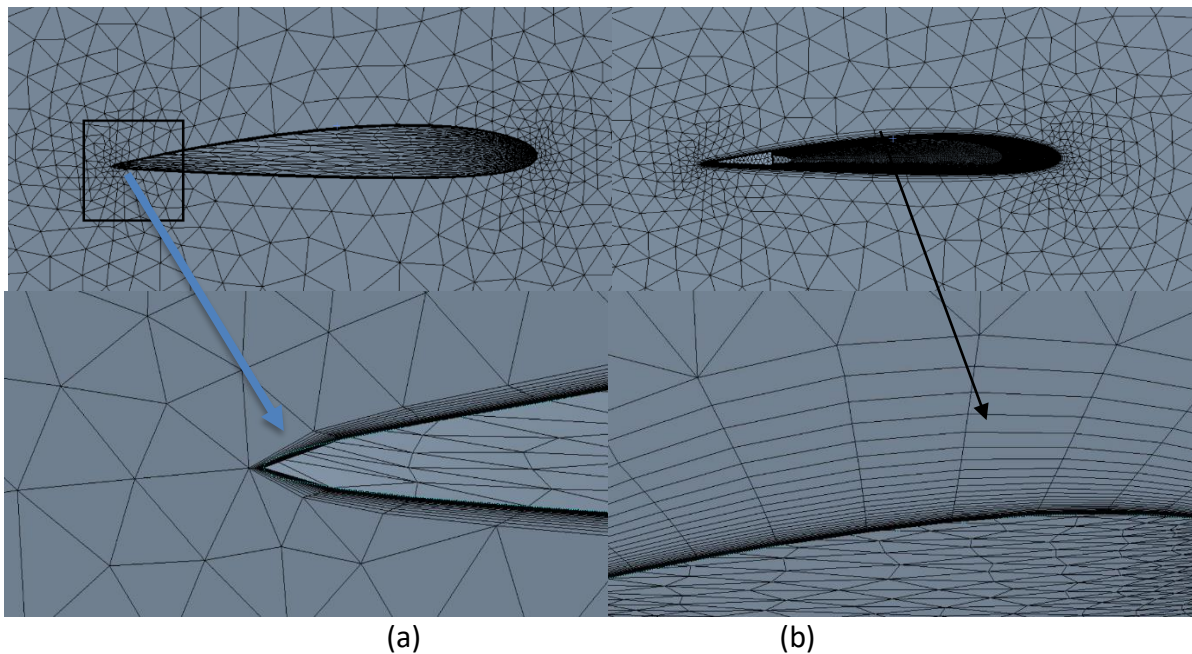


Fig. 6. Mesh generation (a) Mesh around the wing with domain (b) Inflation layer

2.3 Governing Equations

In the context of steady-state external aerodynamics, ANSYS Fluent addresses the governing equations mass conservation, commonly referred to as the continuity equation. This process involves ensuring that the mass entering and leaving any given volume within the flow field remains balanced, thereby satisfying the principles of fluid dynamics: $\nabla \cdot (\rho \vec{v}) = 0$ and for momentum [22]:

$$\nabla \cdot (\rho \vec{v} \vec{v}) = -\nabla p + \nabla \cdot (\tau)$$
(1)

Anderson provides the comprehensive system of governing equations and their fundamental physical principles. The treatment of compressible viscous flow density adheres to the ideal gas law: $\rho = P_{abs} / (R/MwT)$, The viscosity was determined using the Sutherland approximation method [23]:

$$\mu/\mu_0 = T_{ref} + S/T + S(T/T_{ref})^n \tag{2}$$

2.4 Formulation of the Problem

The corporate CFD software Ansys Fluent 19.2 has been utilized to perform numerical simulations of the external flow aerodynamics. To achieve accurate results, the software employs a second-order central difference approach for interpolating diffusive terms from their cell-centred values to the face positions. The gradients at cell centres are calculated using the least squares cell-based reconstruction method, which enhances the accuracy of the gradient estimation. Additionally, a limited multidimensional gradient approach is implemented to prevent non-physical oscillations and numerical instabilities, ensuring the robustness and reliability of the simulation results. This sophisticated numerical scheme allows for a detailed and accurate analysis of the aerodynamic performance under various flow conditions.

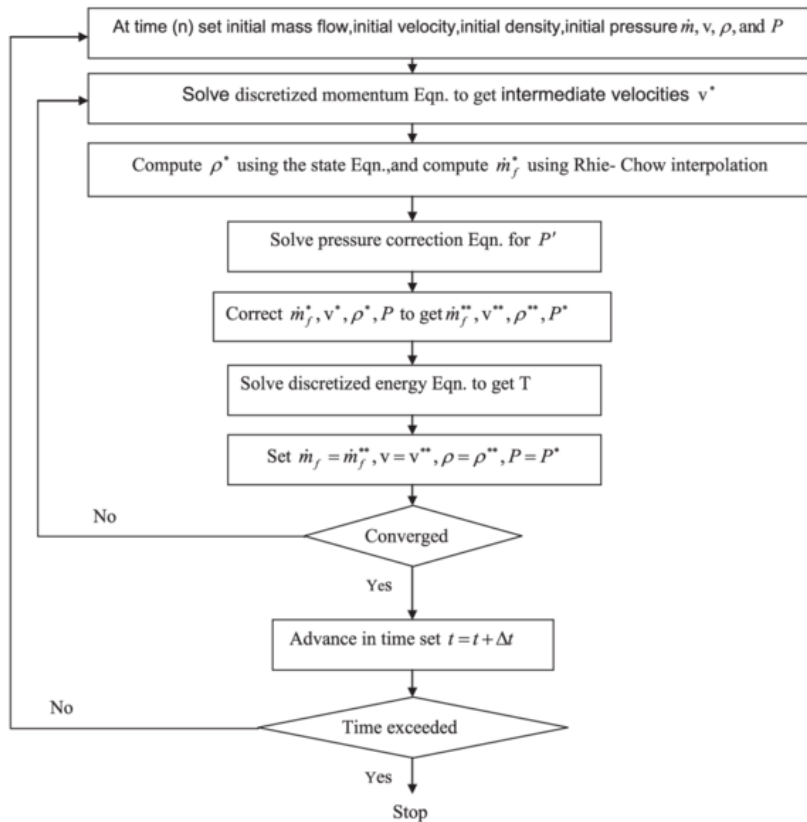


Fig. 7. SIMPLE Algorithm flow chart

The SIMPLE Algorithm method is employed to achieve pressure-velocity coupling, utilizing the default under-relaxation settings. To avoid pressure checkerboard instability, the Rhie-Chow interpolation technique is used, particularly effective because the solution is computed on collocated meshes. For turbulence modelling, the $k-\omega$ SST (Shear Stress Transport) model is chosen. This decision follows an evaluation of several RANS (Reynolds-Averaged Navier-Stokes) CFD models, including the Spalart-Allmaras, $k-\epsilon$ and $k-\omega$ SST models. The $k-\omega$ SST model is selected for its superior

ability to accurately represent turbulence effects, particularly in predicting higher-order stress relaxation terms. The $k-\omega$ SST model effectively captures the near-wall viscous sublayer demanding $k-\epsilon$ model in the regions adjacent to the wall, providing detailed resolution of the boundary layer [6,7]. For far-field applications, it utilizes the $k-\omega$ model, which is less resource-intensive, thereby optimizing computational resources while maintaining high flow resolution. The current study resolves the steady-state Reynolds-Averaged Navier-Stokes (RANS) equations in three dimensions to obtain the solution. The mathematical formulation of the two-equation turbulence model used in this study is illustrated in Figure 7. This sophisticated approach ensures a comprehensive and accurate simulation of the aerodynamic performance, taking full advantage of the $k-\omega$ SST model's capabilities to handle complex turbulent flows.

Turbulence Kinetic Energy

$$\frac{\partial}{\partial t}(\rho k) + \frac{\partial}{\partial x_j}(\rho k u_j) = P - \beta^* \rho \omega k + \frac{\partial}{\partial x_j} \left[(\mu + \sigma_k \mu_t) \frac{\partial k}{\partial x_j} \right] \quad (3)$$

Specific Dissipation Rate

$$\frac{\partial}{\partial t}(\rho \omega) + \frac{\partial}{\partial x_j}(\rho \omega u_j) = \frac{\gamma}{\sigma_t} P - \beta \rho \omega^2 k + \frac{\partial}{\partial x_j} \left[(\mu + \sigma_\omega \mu_t) \frac{\partial \omega}{\partial x_j} \right] + 2(1 - F_1) \sigma_\omega^2 \frac{1}{\omega} \frac{\partial k}{\partial x_i} \frac{\partial \omega}{\partial x_i} \quad (4)$$

The source publications are taken from the previous study [5-7] provide comprehensive definitions of all terminology used in the Eq. (3) and Eq. (4).

2.5 Computation Set Up

The fundamental governing equations of fluid dynamics—the continuity, momentum and energy equations are used to compute the flow analysis. The boundaries of the computational domain extend six times larger than the dimensions of the design. The wing's outer surface is treated as a no-slip fixed wall, while the enclosure's edges are considered walls without shear. By doing this, the computational error caused by an absence of assets for addressing a vast air region is significantly decreased. The ordinary threshold of the airflow region in ahead of the aircraft wing's leading edge is given an intake speed of 40 m/s were taken from previous study by Narayan *et al.*, [4], this is typical for a plane with wings of equal size. To accommodate low-altitude flight conditions where the wing is more prone to stalling, a turbulence intensity of 5% was applied at standard temperature and pressure (STP). At the exit of the flow domain, the external air pressure is set to zero-gauge pressure.

Table 3
 Boundary conditions

Parameter	Types
Solver	Pressure based
Turbulence model	K-omega, SST
No slip wall	Wing with and without winglets
Domain	Rectangular
Taper Ratio	0.8
Re	6.7×10^6
Mach Number	0.1

In this modelling the flow characteristics, the simulation was carried out in standard atmospheric conditions with inlet pressure, temperature, density and viscosity as 101325 Pa, 288 K, 1.225 Kg/m³ and 1.805 x 10⁻⁵ Kg/m s with certain SIMPLE algorithm and second order upwind discretization scheme applied as illustrated in Table 3.

The coefficient of lift of the present study with velocity 30 m/s and as per literature survey parameters [21] were compared with the experiment result which was taken at velocity 30 m/s with similar Mach number 0.9 and Reynolds number 5 x 10⁵ as shown in Table 4. Then the present study velocity was changed to 40 m/s [4] as per the comparison shows nearly equal to the experimental values with less error. Applying statistical significance tests, such as ANOVA or t-tests, to compare the aerodynamic performance of different winglet configurations could provide a more rigorous basis for the claims. These tests would help confirm whether the observed differences in lift and drag between the baseline, raked, blended and corrugated winglets are statistically significant, rather than a result of random variation in the simulation model.

Table 4
 Validation study of numerical (present) with experimental [21]

AOA	Cl Present Simulation	Cl Experiment [21]	% difference
0	0.1975	0.2051	3.70
4	0.7254	0.7557	4.09
8	1.0399	0.9725	6.90
12	1.3570	1.2016	12.90
16	1.5301	1.1911	28.40

The sub-mesh's parameters were set at 20 layers and a growth factor of 1.5. The comparison with wind-tunnel actual data in Figure 8 illustrates the impact of the inflated boundary-layer-resolution structured sub mesh on lift computational results. The solution of the taper wing of NACA 2412 are contrasted in the current study when the model is varied for various winglets, such as raked, blended, CRW and CBW. In this study, the lift and drag coefficients, lift/drag ratios and tip vortices are all investigated.

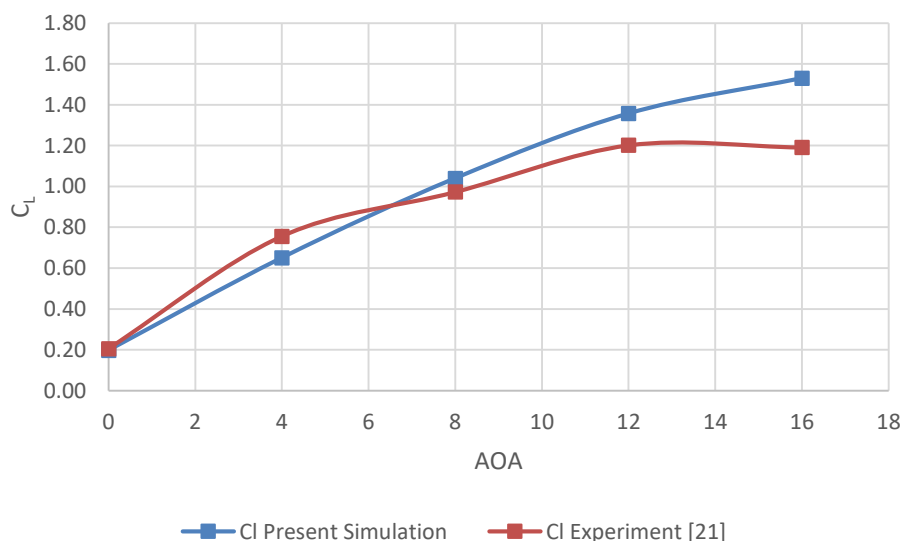


Fig. 8. Comparison between simulation and experiment [21]

3. Result and Discussion

This study examines a 3D wing with and without winglets in five scenarios, including conventional, raked, blended, CRW and CBW winglets, using the finite volume approach. It has been demonstrated that when winglets are placed, the lift coefficient values for CRW and CBW winglets rises and the coefficient of drag falls at greater AOA. Additionally, the lift to drag ratio rises in comparison to other models, notably with the raked and blended winglet. Although blended winglets create greater L/D ratios than raked at an AOA of 8°, 12° and 16°, raked winglets still produce a superior lift coefficient than a conventional wing. Finally, compared to CRW and CBW models, the baseline wing, blended and raked winglets have lower L/D ratios. At angles of attack of 8°, 12° and 16°, the CRW and CBW winglets model provides superior drag reduction than the other type. As the result shows the modified winglets gives the L/D ratio more by using base models like raked and blended winglets. The literature survey of winglets with modification and multi wing tips gives the 5 % more increase in lift when compared to conventional wing. The changes between the CBW models were essentially identical to the blended winglets. Here, it has been determined that, when compared to the current basic raked and blended winglet models, the winglets CBW model and CRW model produce improved results with regard to drag reduction without negatively impacting the lift. These study states a numerical result of the corrugation winglets and base raked and blended winglets were identical in the lift increase and gives impact in the drag reduction.

The drag coefficient vs angle of attack for the winglets built in the current investigation is displayed in Figure 9. As the angle of attack rises, the drag coefficient can be seen to rise. The graph shows the CRW and CBW decrease in drag at higher angle of attack as compared with conventional wing.

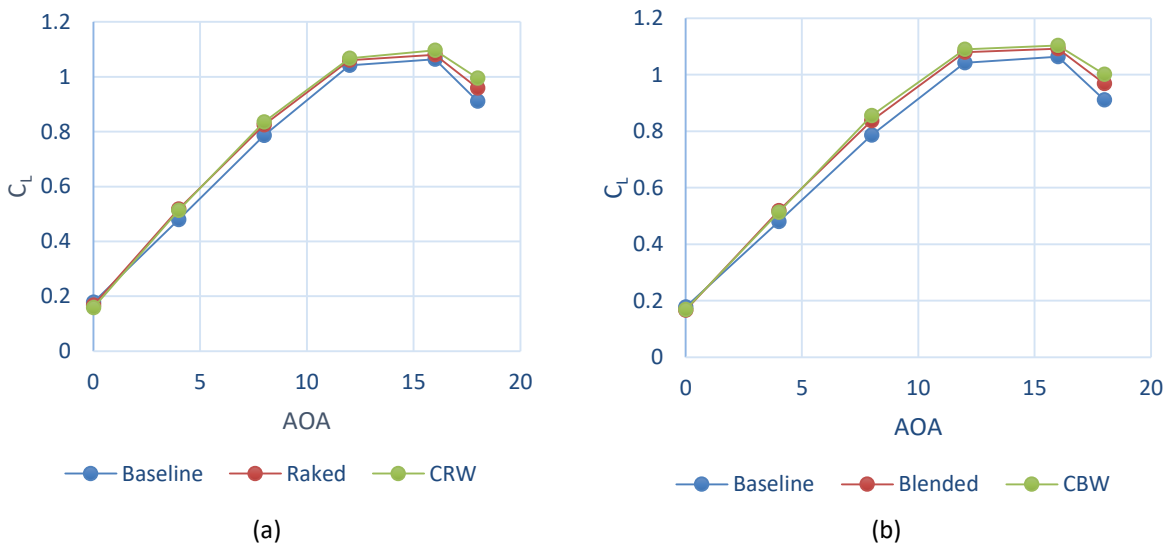


Fig. 9. Comparative lift coefficient graph of raked and blended winglet with conventional wing (a) lift curve of Raked vs CRW (b) lift curve of Blended vs CBW

The coefficient of lift is more in the modified winglets when compared with conventional wing and the base raked and blended winglets at higher angle of attack as shown in Figure 10.

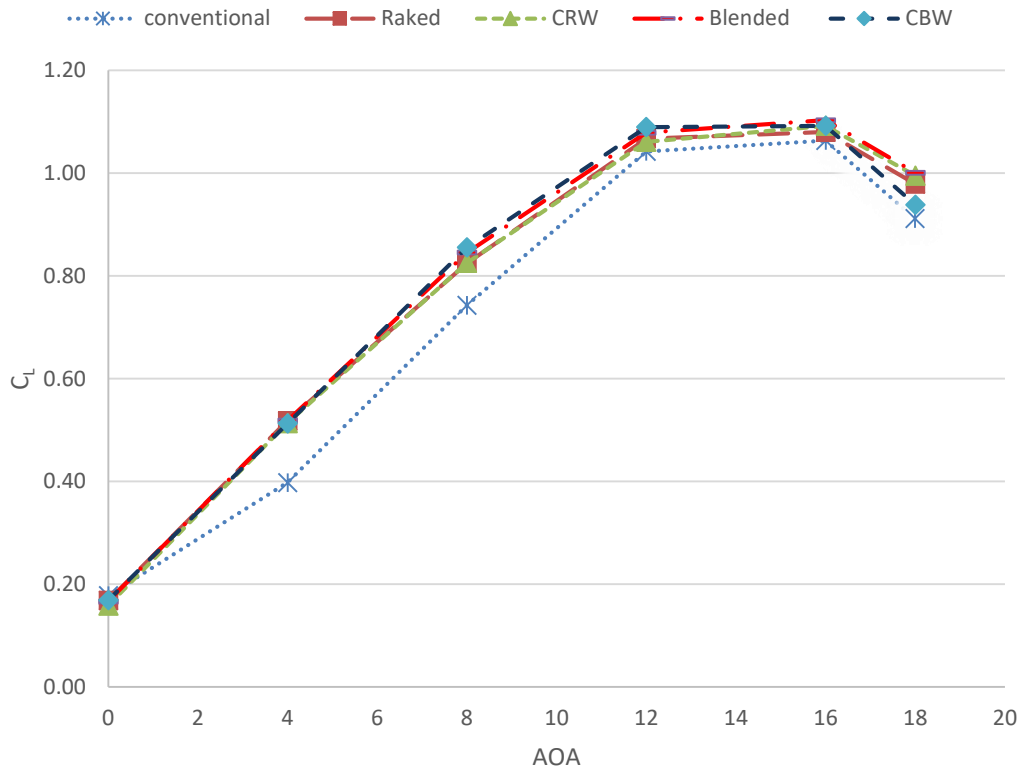


Fig. 10. C_L Vs AOA

The coefficient of drag is less in the modified winglets when compared with conventional wing and the base raked and blended winglets at higher angle of attack as shown in Figure 11.

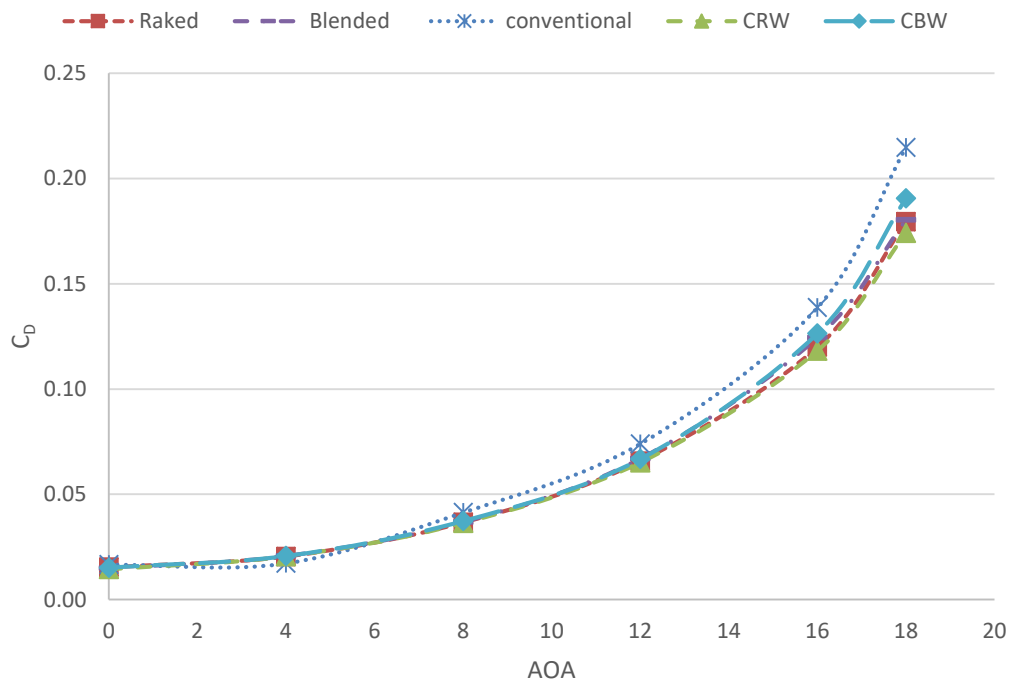


Fig. 11. C_D Vs AOA

The lift to drag ratio is increased in the modified winglets when compared with conventional wing and the base raked and blended winglets at different angle of attack as shown in Figure 12.

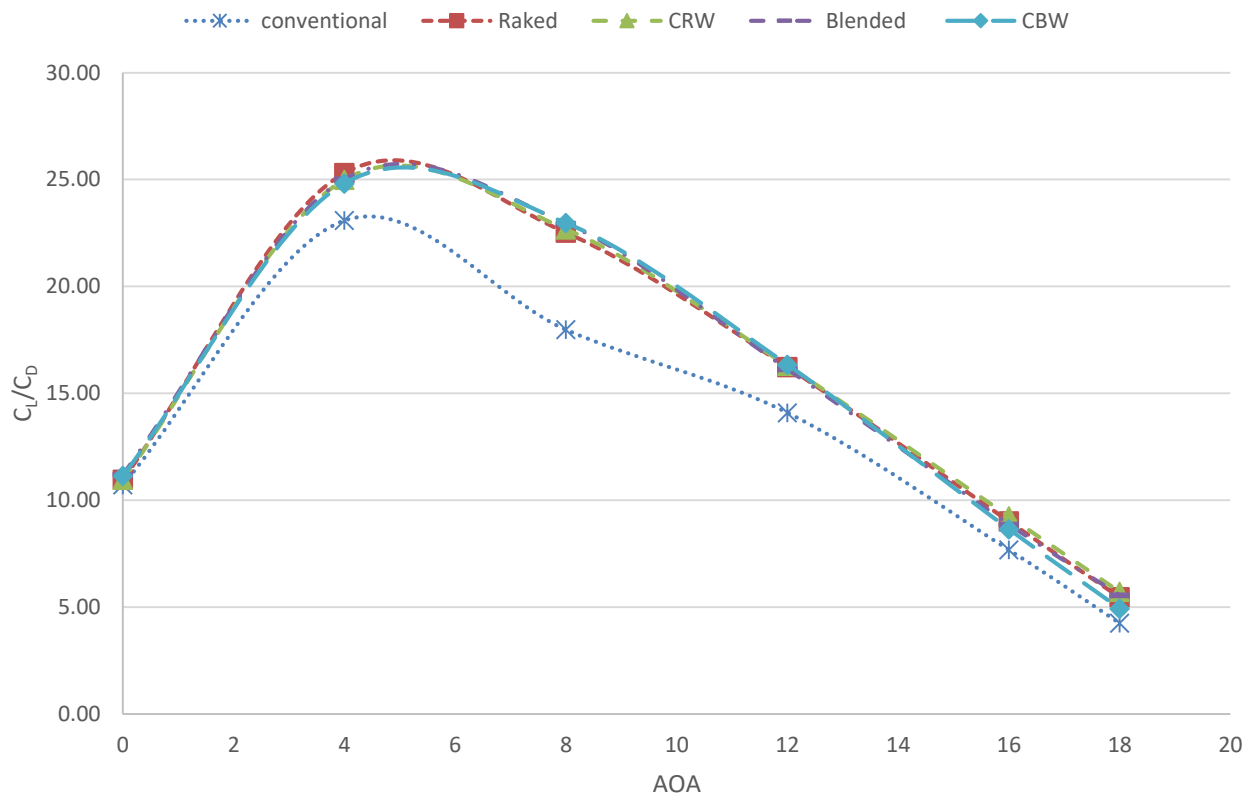
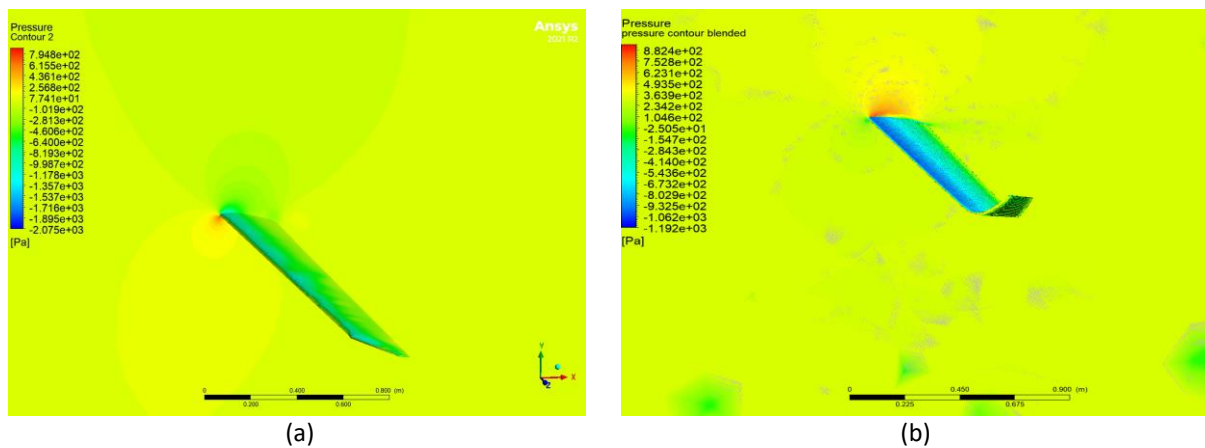


Fig. 12. C_l/C_D Vs AOA

The pressure contour of the CRW and CBW as shown in Figure 13 where the pressure acting at surface area of the wing compared with exit raked and blended model at 4° angles of attack.



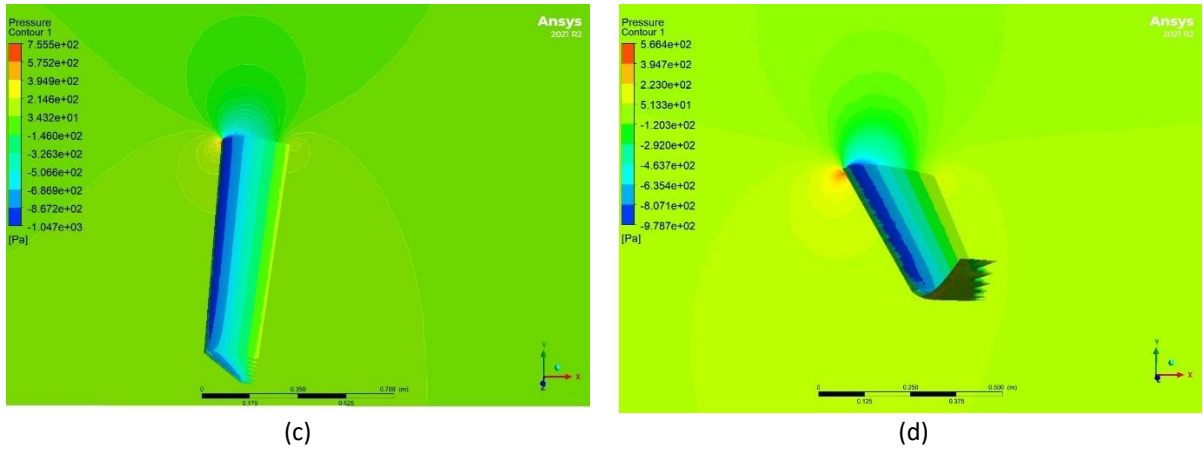


Fig. 13. pressure contour at angle of attack 4° (a) pressure contour of raked winglet (b) pressure contour of blended winglet (c) pressure contour of CRW (d) pressure contour of CBW

The corrugation winglets are highly in contrast with the base winglets in the swirls reduction at the tip as shown in Figure 14 which in the way of amplitude and wavelength interference at the tip produces good impact on swirls reduction without affecting the weight at the cruise conditions.

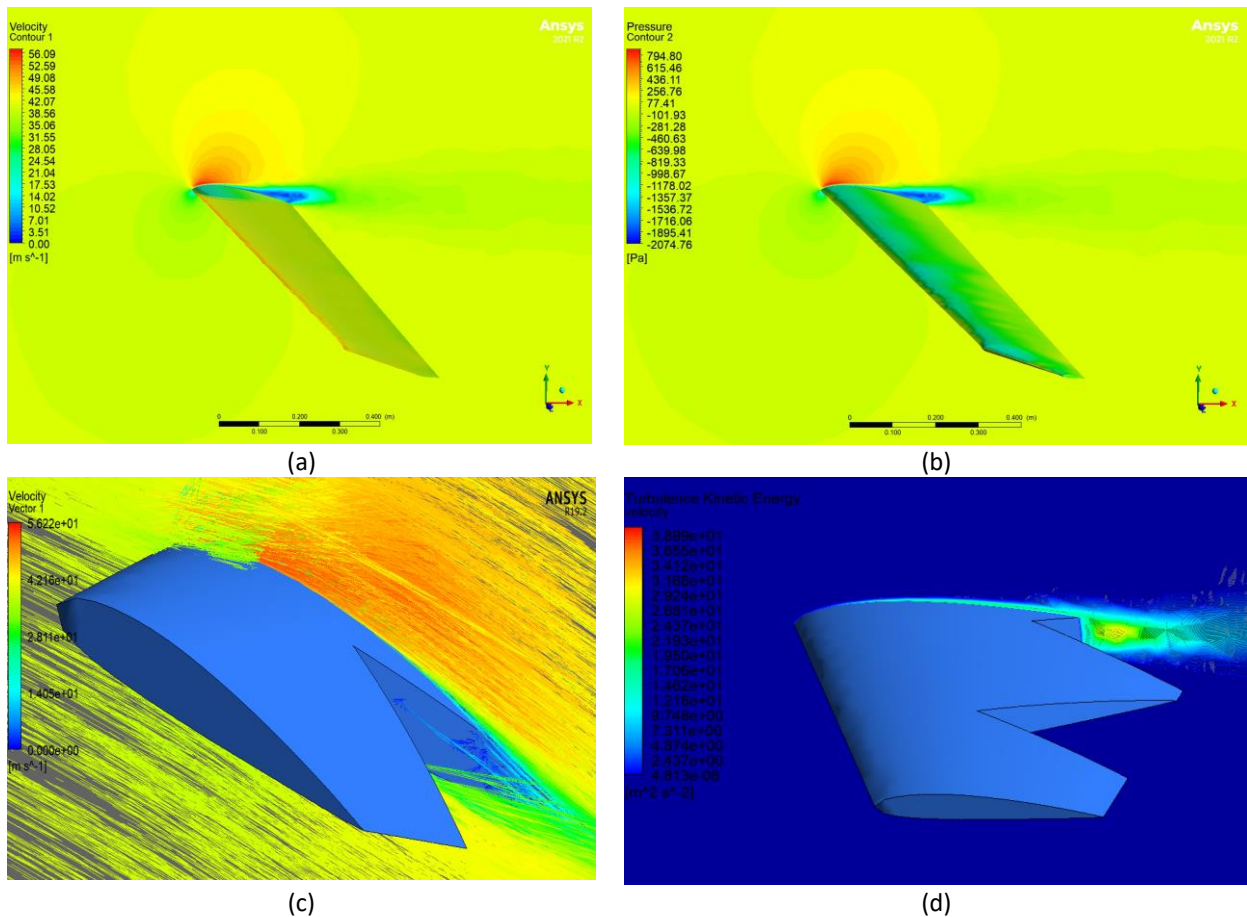


Fig. 14. Sample velocity contour (a) velocity contour of raked winglet (b) velocity contour of raked winglet at 4° AOA (c) velocity vector of CRW (d) turbulent kinetic energy of CBW

4. Conclusions

In conclusion, this research was conducted to determine the performance of the raked and blended winglets with corrugated modification. In summary, corrugation in winglets can improve their structural strength, aerodynamic performance and manufacturing efficiency, contributing to the overall effectiveness of the winglets in reducing drag and enhancing aircraft performance. Corrugated surfaces can sometimes contribute to noise reduction by altering the airflow patterns around the winglet, potentially leading to quieter operations. Corrugations can also improve the aerodynamic performance of winglets. By enhancing the boundary layer control, corrugations can help delay flow separation and reduce drag. This can enhance the overall efficiency of the winglet in reducing wingtip vortices and improving fuel efficiency. The study demonstrates that corrugated winglets provide an improvement in aerodynamic performance, notably in reducing drag and increasing the lift-to-drag ratio compared to conventional wings. The simulation results, as shown in Figures 9, 10 and 13, indicate a 7% improvement in lift for the corrugated winglets (CRW and CBW models) relative to conventional designs. However, to further substantiate these claims, statistical tools can be incorporated to provide more confidence in the results. In order to show the winglet aerodynamic performance, the corrugation is introduced in raked and blended winglets at low-speed condition. Based on the detailed numerical investigation the following conclusions were made as follows:

- i. The lift values of CRW and CBW rises without affecting the existing lift and decreases the drag coefficient at higher angles of attack.
- ii. Notably compare with normal raked and blended winglet model, the modified models give more lift to drag ratio at higher angles of attack.
- iii. According to the present study, the corrugation type of winglets gives 2 % more than the base model of raked and blended winglets which is 7 % more lift without affecting drag when compared with conventional wing at higher angles of attack. Additionally, the aerodynamic characteristics of all the modified model wing configuration tend to increase in the standard turbulence intensity and the angles of attack.

However, addressing real-world manufacturing challenges, cost implications and regulatory considerations would strengthen the practical relevance of these findings:

- i. Corrugation introduces complexity into the design and production processes. Achieving the precise geometrical tolerances needed to optimize aerodynamic performance could increase the difficulty of mass production, especially for large-scale commercial applications. This could require more advanced fabrication techniques, such as 3D printing or precision machining, which may elevate production costs.
- ii. While the improved aerodynamic performance (e.g., 7% lift increase and drag reduction) could offer fuel savings over time, the initial investment in advanced manufacturing methods might offset these gains. A comprehensive cost-benefit analysis, including manufacturing costs, maintenance and operational savings, would help quantify the financial viability of implementing corrugated winglets in commercial aircraft.
- iii. The implementation of any new winglet design, including corrugated winglets, must comply with aviation safety standards and certifications. Regulatory bodies such as the Federal Aviation Administration (FAA) and the European Union Aviation Safety Agency (EASA) have strict guidelines on aircraft modifications. The structural integrity of the

corrugated design, its impact on overall flight dynamics and potential acoustic effects (e.g., noise reduction) need to be validated through extensive testing and certification processes before these designs can be approved for commercial use.

5. Future Work

This study involves the numerical analysis of corrugated raked and blended winglets, focusing on aerodynamic performance. While the findings are promising, several limitations should be acknowledged:

- i. The simulations were conducted under idealized conditions (e.g., steady-state flow, fixed atmospheric conditions and no structural deformation). Real-world factors such as atmospheric turbulence, structural flexibility and changing environmental conditions were not fully integrated into the model. These assumptions may affect the accuracy of the predictions in practical applications.
- ii. The winglet designs analysed in this study are based on specific corrugation dimensions and fixed geometric configurations. Variations in these parameters, such as changing the amplitude or wavelength of the corrugations or testing different aspect ratios, were not explored. Future work should examine a broader range of winglet shapes and corrugation patterns to determine the most effective configurations under various flight conditions.
- iii. The current analysis is purely numerical and while it provides insight into aerodynamic trends, experimental validation is essential to confirm the accuracy of the simulations. Wind tunnel testing and real-flight experiments should be performed to validate the predicted improvements in lift and drag reduction, as well as to assess the structural integrity of corrugated winglets under operational loads.
- iv. Noise reduction, particularly from wingtip vortices, was not directly analysed in this study, although it is a critical factor in the evaluation of winglets. Further studies should include acoustic simulations and testing to assess the potential noise-reduction benefits of corrugated winglets.

Acknowledgement

This research was not funded by any grant.

References

- [1] Anderson, John. *EBOOK: Fundamentals of Aerodynamics (SI units)*. McGraw hill, 2011.
- [2] Whitcomb, Richard T. *A design approach and selected wind tunnel results at high subsonic speeds for wing-tip mounted winglets*. No. L-10908. 1976.
- [3] McLean, Doug. "Wingtip devices: what they do and how they do it." In *Boeing performance and flight operations engineering conference*. 2005.
- [4] Narayan, Gautham and Bibin John. "Effect of winglets induced tip vortex structure on the performance of subsonic wings." *Aerospace Science and Technology* 58 (2016): 328-340. <https://doi.org/10.1016/j.ast.2016.08.031>
- [5] Wilcox, D. C. "Turbulence Modeling for CFD." *DCW industries, La Canada* (1998).
- [6] Menter, Florian. "Zonal two equation kw turbulence models for aerodynamic flows." In *23rd fluid dynamics, plasmadynamics and lasers conference*, p. 2906. 1993. <https://doi.org/10.2514/6.1993-2906>
- [7] Menter, Florian R. "Two-equation eddy-viscosity turbulence models for engineering applications." *AIAA journal* 32, no. 8 (1994): 1598-1605. <https://doi.org/10.2514/3.12149>
- [8] Abbott, Ira H. and Albert E. Von Doenhoff. *Theory of wing sections: including a summary of airfoil data*. Courier Corporation, 2012.
- [9] Hicken, Jason E. and David W. Zingg. "Induced-drag minimization of nonplanar geometries based on the Euler equations." *AIAA journal* 48, no. 11 (2010): 2564-2575. <https://doi.org/10.2514/1.J050379>

- [10] Shollenberger, C. A. *Application of an optimized winglet configuration to an advanced commercial transport*. No. NASA-CR-159156. 1979.
- [11] Smith, Leigh Ann. *Effects of winglets on the drag of a low-aspect-ratio configuration*. Vol. 3563. NASA, Langley Research Center, 1996.
- [12] Halpert, Joel, Daniel Prescott, Thomas Yechout and Michael Arndt. "Aerodynamic optimization and evaluation of KC-135R winglets, raked wingtips and a wingspan extension." In *48th AIAA Aerospace Sciences Meeting Including the New Horizons Forum and Aerospace Exposition*, p. 57. 2010. <https://doi.org/10.2514/6.2010-57>
- [13] Juknevičius, Auris, Tze Pei Chong and Philip C. Woodhead. "Leading edge noise reduction of thin aerofoil by the straight and curved serrations of the add-on type." In *23rd AIAA/CEAS Aeroacoustics Conference*, p. 3491. 2017. <https://doi.org/10.2514/6.2017-3491>
- [14] Nedić, J. and J. Christos Vassilicos. "Vortex shedding and aerodynamic performance of airfoil with multiscale trailing-edge modifications." *AIAA Journal* 53, no. 11 (2015): 3240-3250. <https://doi.org/10.2514/1.J053834>
- [15] Gueraiche, Djahid and Sergey Popov. "Winglet geometry impact on DLR-F4 aerodynamics and an analysis of a hyperbolic winglet concept." *Aerospace* 4, no. 4 (2017): 60. <https://doi.org/10.3390/aerospace4040060>
- [16] Guerrero, Joel, Marco Sanguineti and Kevin Wittkowski. "CFD study of the impact of variable cant angle winglets on total drag reduction." *Aerospace* 5, no. 4 (2018): 126. <https://doi.org/10.3390/aerospace5040126>
- [17] Hariyadi, SP Setyo, Wawan Aries Widodo and Imam Sonhaji. "Numerical study of secondary flow characteristics on the use of the winglets." In *Journal of Physics: Conference Series*, vol. 1726, no. 1, p. 012012. IOP Publishing, 2021. <https://doi.org/10.1088/1742-6596/1726/1/012012>
- [18] Shahzad, A., H. R. Hamdani and Ahmad Aizaz. "Investigation of corrugated wing in unsteady motion." *Journal of Applied Fluid Mechanics* 10, no. 3 (2017): 833-845. <https://doi.org/10.18869/acadpub.jafm.73.240.26425>
- [19] Rohmawati, Iis, Hiroshi Arai, Hidemi Mutsuda, Takuji Nakashima and Rizal Mahmud. "Optimizing Effect of Wavy Leading Edge (WLE) in Rectangular Wing and Taper Wing." *Journal of Mechanical Engineering, Science and Innovation* 1, no. 2 (2021): 56-68. <https://doi.org/10.31284/j.jmesi.2021.v1i2.2296>
- [20] Ilie, Marcel, Matthew White, Valentin Soloiu and Mosfequr Rahman. "The effect of winglets on the aircraft wing aerodynamics; numerical studies using LES." In *AIAA Scitech 2019 Forum*, p. 1308. 2019. <https://doi.org/10.2514/6.2019-1308>
- [21] Matsson, John E., John A. Voth, Connor A. McCain and Connor McGraw. "Aerodynamic performance of the NACA 2412 airfoil at Low Reynolds Number." In *2016 ASEE Annual Conference & Exposition*. 2016.
- [22] Fluent, A. N. S. Y. S. "Ansys fluent theory guide." *Ansys Inc., USA* 15317 (2011): 724-746.
- [23] Anderson, John. *EBOOK: Fundamentals of Aerodynamics (SI units)*. McGraw hill, 2011.
- [24] Zhang, Liang, M. A. Dongli, Y. A. N. G. Muqing and W. A. N. G. Shaoqi. "Optimization and analysis of winglet configuration for solar aircraft." *Chinese Journal of Aeronautics* 33, no. 12 (2020): 3238-3252. <https://doi.org/10.1016/j.cja.2020.04.008>
- [25] Nafi, Asif Shahriar, Nikolaos Beratlis, Elias Balaras and Roi Gurka. "Numerical study of owls' leading-edge serrations." *Physics of Fluids* 35, no. 12 (2023). <https://doi.org/10.1063/5.0174145>
- [26] Kharis, Rinal and Harinaldi Harinaldi. "Investigating the Effects of Vortex Generator Geometry on NACA Inlet Performance." *CFD Letters* 17, no. 1 (2025): 17-34. <https://doi.org/10.37934/cfdl.17.1.1734>
- [27] Kamal, Nur Nabillah Mohd, Adi Azriff Basri, Ernie Illyani Basri, Ida Suriana Basri and Mohd Firdaus Abas. "Comparison study between Schrenk's approximation method and computational fluid dynamics of aerodynamic loading on UAV NACA 4415 wing." *Journal of Advanced Research in Fluid Mechanics and Thermal Sciences* 64, no. 2 (2019): 283-292.
- [28] Arafat, Mohammad, Izuan Amin Ishak, Muhammad Aidil Safwan Abdul Aziz andrew Wee Shong Soh, Woei Ting Tiong, Nur Rasyidah Roziman, Nur Amiza Mohd Hairul et al., "A Hybrid RANS/LES Model for Predicting the Aerodynamics of Small City Vehicles." *Journal of Advanced Research in Experimental Fluid Mechanics and Heat Transfer* 17, no. 1 (2024): 1-13. <https://doi.org/10.37934/arefmht.17.1.113>